On the Annual Cycle of the Eastern Equatorial Pacific

TIANMING LI AND S. GEORGE H. PHILANDER

Atmospheric and Oceanic Sciences Program, Princeton University, Princeton, New Jersey

(Manuscript received 13 January 1995, in final form 2 May 1995)

ABSTRACT

Although the sun "crosses" the equator twice a year, the eastern equatorial Pacific has a pronounced annual cycle, in sea surface temperature and in both components of the surface winds for example. (This is in contrast to the Indian Ocean and western Pacific where a semiannual oscillation of the zonal wind is the dominant signal on the equator.) Calculations with a relatively simple coupled ocean–atmosphere model indicate that the principal reason for this phenomenon is the marked asymmetry, relative to the equator, of the time-averaged climatic conditions in the eastern tropical Pacific. The important asymmetries are in surface winds, oceanic currents, and sea surface temperature: The time-averaged winds and currents have northward components at the equator and the warmest waters are north of the equator. Because of those asymmetries, seasonally varying solar radiation that is strictly antisymmetric relative to the equator can force a response that has a symmetric component. The amplitude of the resultant annual cycle at the equator depends on interactions between the ocean and atmosphere, and on positive feedbacks that involve low-level stratus clouds that form over cold surface waters.

1. Introduction

Although the sun "crosses" the equator twice a year, an annual harmonic is dominant in the sea surface temperature variations of the eastern tropical Pacific and Atlantic. Figure 1 shows that the phase of this annual cycle is that of the seasons of the Southern Hemisphere—temperatures are at a maximum toward the end of the southern summer—and that the temperature and zonal wind fluctuations are highly correlated on the equator at 110°W and 30°W. The correlation is negligible at the island Gan (0°, 70°E) in the central Indian Ocean where a semiannual signal dominates the zonal wind variations. Figure 2 offers another perspective on the special character of the seasonal cycle in the eastern tropical Pacific and Atlantic, and on the contrast between oceanic and continental variations. It shows conditions close to the extremes of the seasonal cycle. In October, sea surface temperatures at and to the south of the equator are low, the intense southeast trades cross the equator, and the intertropical convergence zone is farthest north. That is not the case over the continents where the maximum cloudiness has already moved southward and is near the equator (because October is close to the equinox). During the subsequent months, as the sun "moves" farther south, it carries the continental convective zones with it, but over the waters of the eastern tropical Pacific and Atlantic the ITCZ remains in a northerly position. By April, long after the southern solstice, the waters south of the equator have warmed sufficiently for the ITCZ to move toward the equator (Mitchell and Wallace 1992).

There is little difficulty in explaining the annual cycle near the equator if we take a strictly atmospheric point of view and regard changes in the temperature of the surfaces below the atmosphere as given. Those temperature changes strongly affect the atmosphere and, in part, are responsible for the seasonal changes in atmospheric conditions. The two following mechanisms are of particular importance over the eastern tropical Pacific and Atlantic: 1) pressure gradients in the lower atmosphere created by the sea surface temperature gradients (Lindzen and Nigam 1987) and 2) movements of the convective zones that remain over the warmest waters and onto which the winds converge (Matsuno 1966; Gill 1980). If the warmest waters, and hence the convective zone onto which the northeast and southeast trades converge, move back and forth across the equator as in the western Pacific, then at the equator the zonal winds will have a semiannual cycle. If, however, the warmest water is always north of the equator so that the ITCZ is always north of the equator, as is usually the case in the eastern Pacific, then the southeast trades always prevail near the equator. Their intensity fluctuates from intense to weak so that, at the equator, both components of the wind have an annual cycle. Thus, the annual fluctuations in sea surface temperatures near the equator can translate into annual variations in the winds and other meteorological parameters.

From an oceanic point of view the annual harmonic in sea surface temperature at the equator is attributable

Corresponding author address: Dr. Tianming Li, Naval Research Laboratory, 7 Grace Hopper Ave., Monterey, CA 93943.
E-mail: li@nrlmry.navy.mil

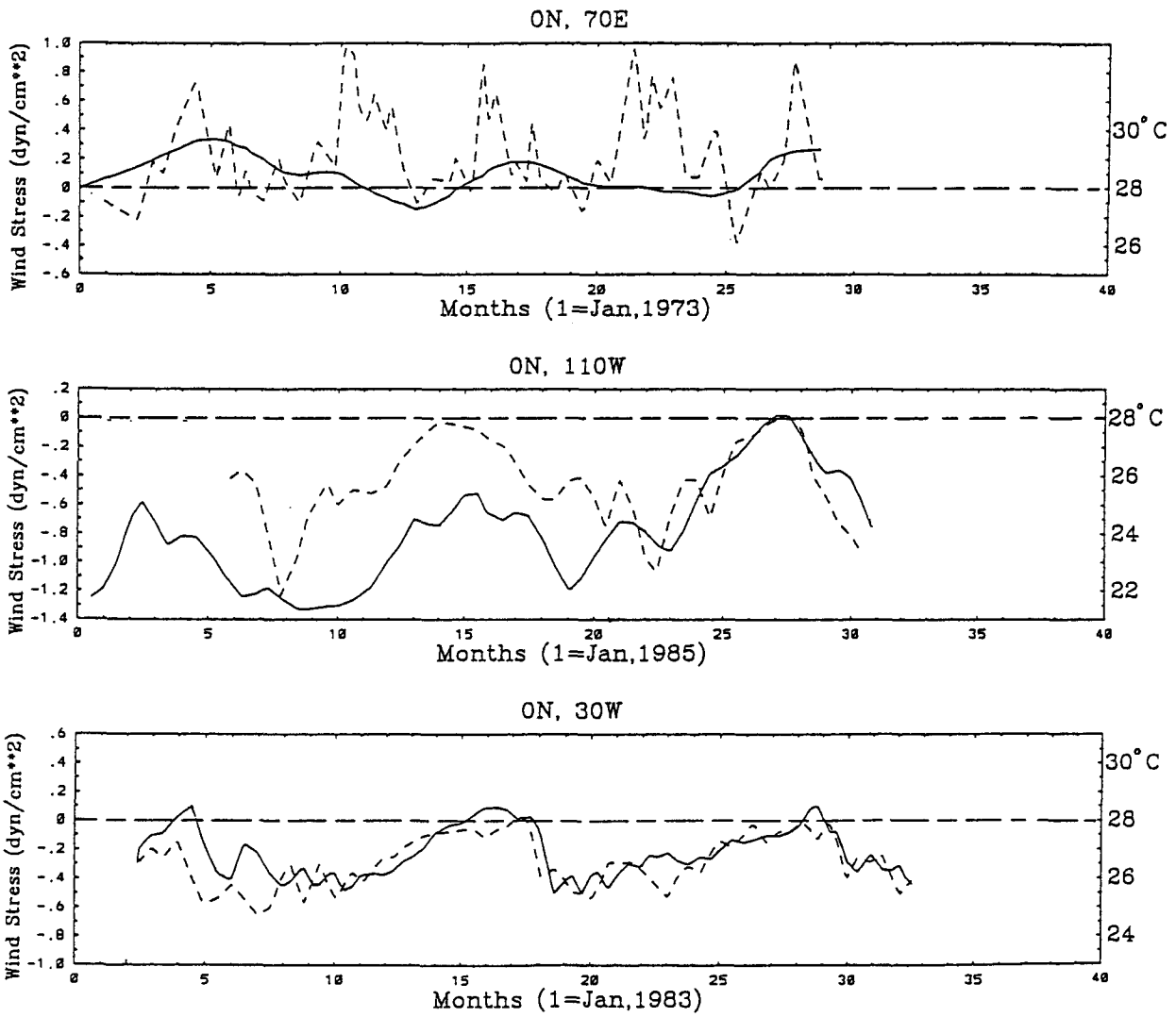

FIG. 1. The time series measurements of sea surface temperature (in °C: solid line) and of the zonal component of the wind stress (in dyn cm^2: dashed line). Time (in units of months) starts on 1 January in all three cases. The first year is (a) 1973 for the measurements at Gan in the Indian Ocean (70°W) by Knox (1981), (b) 1985 for those at 110°W by Halpern (1987) and McPhaden and McCarty (1992), and (c) 1983 for those in the Atlantic at 30°W by Weingartner and Weisberg (1991).

to the annual variations in the surface winds and heat fluxes. Whereas interannual sea surface temperature changes depend on a large-scale horizontal redistribution of warm surface waters in the Tropics and are almost adiabatic, the seasonal changes depend strongly on the local heat fluxes at the ocean surface and on the divergence of the surface currents (Chang 1994; Koeberle and Philander 1994). The heat flux, which is determined primarily by evaporation and shortwave radiation into the ocean, varies annually at the equator because the winds and cloudiness near the equator vary annually. The winds not only cause evaporation but also induce seasonal upwelling that affects sea surface temperatures. The easterly component of the winds induces equatorial upwelling; the southerly component of the winds induces a cross-equatorial cell with upwelling that is most intense just south of the equator (Moore and Philander 1977).

This circular argument that near the equator the annual cycle in sea surface temperatures both causes and results from the annual variations in atmospheric conditions (winds and cloudiness) suggests that ocean–atmosphere interactions influence the earth's response to the seasonal variations in solar radiation. The challenge is to explain how the solar forcing causes the changes in winds, cloudiness, and sea surface temperature. The variations in solar radiation do have an annual harmonic at the equator because the earth's orbit is elliptical rather than circular. Does that annual variation have a sufficient amplitude to cause the observed

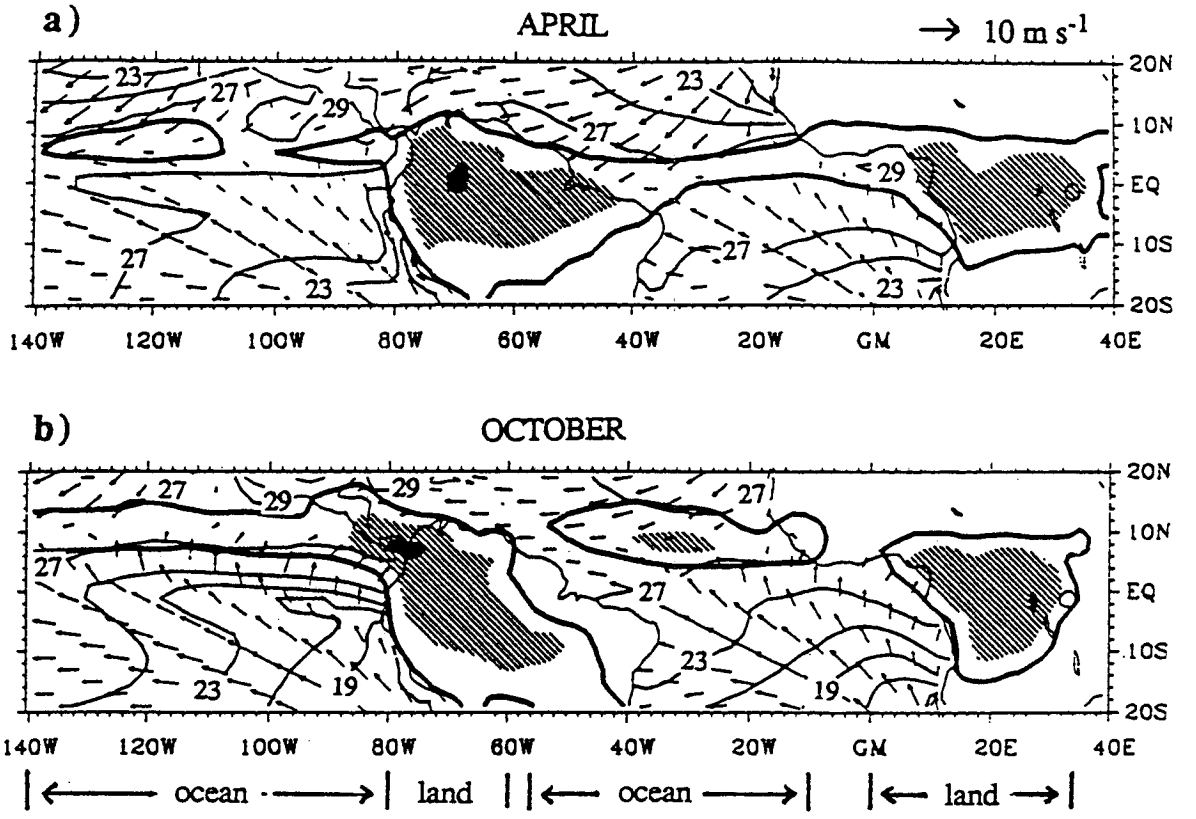

FIG. 2. Western sector OLR, vector surface wind, and SST for (a) April and (b) October. The heavy contour denotes OLR values of 240 W m^{-2}, and light (dark) shading indicates OLR values between 220 and 200 W m^{-2} (<200 W m^{-2}). The SST contour interval is 2°C. Surface winds with wind speeds <1 m s^{-1} are not plotted. The brackets at the bottom indicate longitudes bands in which the seasonal march of northern tropical convection is dominated by oceanic or land convection regimes (adopted from Mitchell and Wallace 1992).

response? The tilt of the earth's axis to the plane of its orbit also causes an annual variation in solar radiation, but it is antisymmetric about the equator and vanishes there. This annual variation can nonetheless force a response at the equator, provided there is an asymmetry in the time-averaged conditions—asymmetries that ultimately are caused by the distribution of land surfaces on the globe.

Two sets of factors contribute to the asymmetry of the time-mean conditions (Philander et al. 1996): The distribution and shapes of continents, which are responsible for modest asymmetries, and ocean–atmosphere interactions plus various feedbacks (some of which involve stratus clouds), which amplify those asymmetries. The relevant ocean–atmosphere interactions are the so-called "slow sea surface temperature" modes that have been explored by Neelin (1991) for the case of symmetry about the equator and by Chang and Philander (1994) for the case of antisymmetry about the equator. Their key feature is the dependence of sea surface temperature changes on divergent oceanic currents. (Vertical displacements of the thermocline are of secondary importance.) Such air–sea interactions require that the winds readily influence the sea surface temperatures (which in turn influence the winds). This is difficult in the western equatorial Pacific where the thermocline is deep but is easy in the eastern equatorial Pacific and Atlantic where the thermocline is shallow. That is why the latter regions have pronounced climatic asymmetries relative to the equator. The reason for a shallow equatorial thermocline in some equatorial regions but not others is the presence of easterly trade winds in some regions (the Atlantic and Pacific) but not in others (the Indian Ocean). The global distribution of continents determines where monsoons and trade winds prevail and, in that manner, determines why the eastern tropical Pacific and Atlantic are regions where modest asymmetries can be amplified.

Next it is necessary to explain which aspect of the continental geometry favors the ITCZ and the warmest surface waters in the Northern rather than Southern Hemisphere. An obvious candidate is the larger land surface area of the Northern Hemisphere. However, calculations with coupled ocean–atmosphere general circulation models, in which the forcing is the time-mean solar radiation, indicate that this is a negligible

factor. Of greater importance is the inclination of the western coast of the Americas to longitude lines and the bulge of western Africa to the north of the Gulf of Guinea. Those details of the local coastal geometries in the eastern Pacific and Atlantic introduce asymmetries that favor an ITCZ north of the equator—asymmetries that are amplified by ocean–atmosphere interactions and other feedbacks (Philander et al. 1996). Can the coastal geometries also cause a nonzero response at the equator to the annual variation in solar radiation associated with the tilt of the earth's axis? Or are asymmetries of the time-mean climate responsible for the annual harmonic at the equator?

This paper is an investigation of the annual cycle at the equator by means of a coupled ocean–atmosphere model that calculates the response to seasonally varying solar radiation but that requires time-averaged conditions to be specified. We can therefore explore the relative importance of asymmetries of coastal geometry and of time-averaged oceanic and atmospheric conditions. The model is discussed in section 2. Section 3 is devoted to a description of the results of various numerical experiments, and section 4 summarizes and discusses the conclusions.

2. The model

The coupled ocean–atmosphere model has as its atmospheric component Lindzen and Nigam's (1987) boundary layer model and as its oceanic component a Cane–Zebiak type model (Cane 1979; Zebiak and Cane 1987).

The oceanic model describes the linear dynamics of a homogeneous, reduced-gravity upper ocean with a varying thermocline. A constant mixed layer is added to the upper ocean. The vertical entrainment velocity at the base of the mixed layer is determined by the Ekman divergence of the surface currents. This type of model has been used widely in studies of the Southern Oscillation (e.g., Zebiak and Cane 1987; Battisti and Hirst 1989; Neelin 1991) and in studies of the seasonal cycle (e.g., Seager et al. 1988; Chang 1994; Chang and Philander 1994). The dynamic and thermodynamic equations of this model can been written as

$$\frac{\partial \mathbf{v}}{\partial t} + f\mathbf{k} \times \mathbf{v} = -g'\nabla h + \frac{\boldsymbol{\tau}}{\rho H} - r\mathbf{v} + \nu\nabla^2\mathbf{v} \quad (2.1a)$$

$$\frac{\partial h}{\partial t} + H\nabla\cdot\mathbf{v} = -rh + \kappa\nabla^2 h \quad (2.1b)$$

$$\frac{\partial \tilde{\mathbf{v}}}{\partial t} + f\mathbf{k} \times \tilde{\mathbf{v}} = \frac{\boldsymbol{\tau}}{\rho H_1} - r_s\tilde{\mathbf{v}} + \nu\nabla^2\tilde{\mathbf{v}} \quad (2.1c)$$

$$\frac{\partial T}{\partial t} + \mathbf{v}_1\cdot\nabla(\bar{T} + T) + \overline{\mathbf{v}_1}\cdot\nabla T = -[M(\bar{w} + w) - M(\bar{w})]\bar{T}_z - M(\bar{w} + w)T_z + \frac{Q}{\rho C_w H_1} - \alpha T + \kappa\nabla^2 T, \quad (2.1d)$$

where $\mathbf{v}$ and $\tilde{\mathbf{v}}$ denote the mean upper-ocean current and the vertical shear current between the mixed layer and the layer below;

$$\mathbf{v}_1 = \mathbf{v} + \frac{H_2}{H}\tilde{\mathbf{v}}$$

represents the surface current; $H_1 = 25$ m and $H = 150$ m are mean mixed layer and thermocline depths, and $H_2 = H - H_1$; $w = H_1\nabla\cdot\mathbf{v}_1$ is the vertical entrainment velocity at the base of the mixed layer; $M(x) = x$, if $x > 0$, and $M(x) = 0$, otherwise, is the Heaviside function; h denotes the varying thermocline; T is sea surface temperature; T_z is the vertical temperature gradient between surface and subsurface; Q denotes surface heat fluxes associated with solar radiation and latent heat fluxes; g' and ρ represent reduced gravity and the density of the upper ocean; r, r_s, and α represent damping coefficients for momentum and heat, and have the values $r = 1/150$ day^{-1}, $r_s = 1$ day^{-1}, and $\alpha = 1/60$ day^{-1}; and ν and κ stand for diffusion coefficients (3×10^3 m^2 s^{-1}). All quantities in Eq. (2.1) with a bar denote annual-mean values and the others denote departures from the mean. Experiments in which the values of the parameters were altered did not affect the results (to be described in later sections) significantly. For example, a decrease in the value of the dissipation parameter α from (60 day)$^{-1}$ to (180 day)$^{-1}$ had little effect on the structure of the annual cycle; it merely increased the amplitude by some 10%. The large value for r_s reflects strong mixing in a surface "Ekman" layer. For a discussion of this and other parameter values, the reader is referred to Zebiak and Cane (1987), whose model is very similar to this one. One difference between their model and ours is the inclusion of the diffusion term in (2.1c). Its presence permits the specification of coastal boundary conditions: both horizontal velocity components can be forced to vanish at the coast.

The annual-mean surface currents and vertical entrainment velocity at the base of the mixed layer are obtained by forcing the ocean model with the observed climatological annual-mean surface winds. The mean surface temperature and vertical temperature gradient are specified from measurements.

The domain of the model is the tropical Pacific from 30°S to 30°N, 120°E to 80°W. A rectangular boundary is used in most experiments. In the studies of coastal effects, the eastern boundary slopes from the northwest to the southeast. The model has a resolution of 2 degrees in longitude and 1 degree in latitude. Calculations start from a state of no motion.

The sea surface temperature is determined by both the dynamical response of the ocean to the wind

$$\boldsymbol{\tau} = \rho_a C_D[|\mathbf{V} + \bar{\mathbf{V}}|(\mathbf{V} + \bar{\mathbf{V}}) - |\bar{\mathbf{V}}|\bar{\mathbf{V}}] \quad (2.2)$$

and the thermodynamic response to heat fluxes. The latter depends primarily on shortwave radiation, which is modified by clouds, and latent heat flux.

Annual Mean SST and Surface Wind

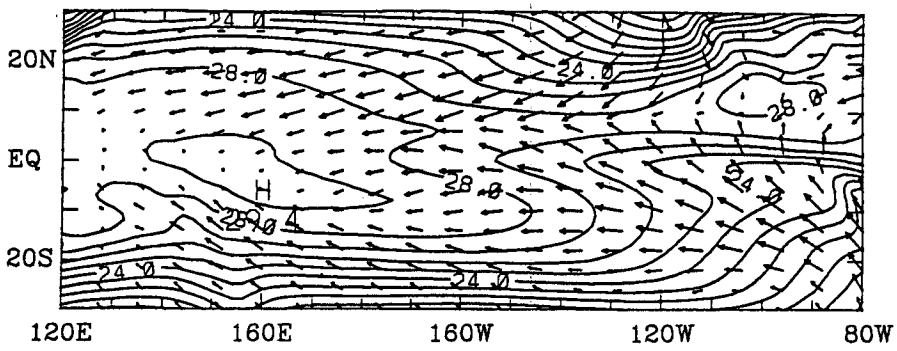

Surface Current and Entrainment Velocity

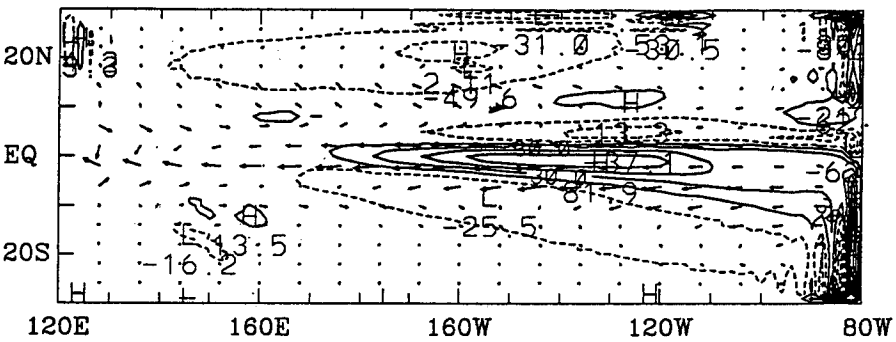

March Simulation

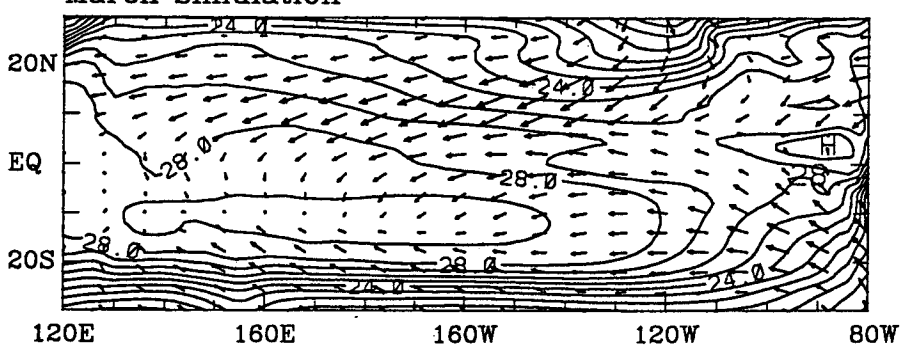

September Simulation

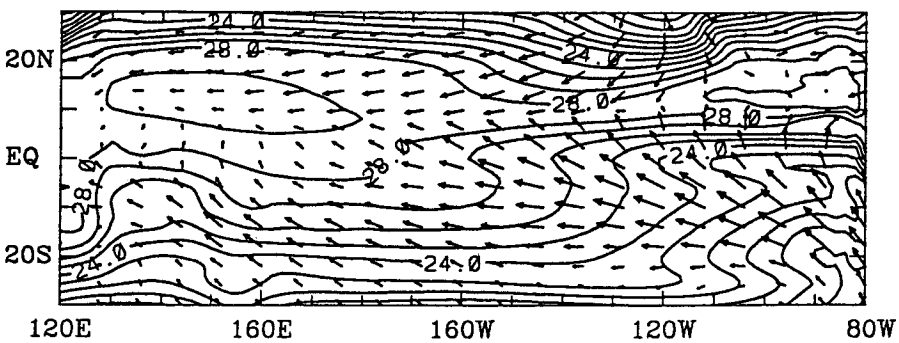

The atmospheric model that is coupled to this oceanic model has to provide the fluctuating part of the winds and the clouds that reduce the shortwave solar radiation. The required winds are calculated by means of the Lindzen–Nigam model for which the equations are as follows:

$$EU - \beta yV = \frac{\partial \phi}{\partial x} + A\frac{\partial T}{\partial x} \tag{2.3a}$$

$$EV + \beta yU = \frac{\partial \phi}{\partial y} + A\frac{\partial T}{\partial y} \tag{2.3b}$$

$$\epsilon\phi = -C_0^2\left(\frac{\partial U}{\partial x} + \frac{\partial V}{\partial y}\right), \tag{2.3c}$$

where U and V are zonal and meridional wind components, ϕ is the geopotential at the top of the atmospheric boundary, E is a boundary-layer friction coefficient, ϵ is an inverse timescale for cumulus convection adjustment; $A = gH_0/2T_0$ and $C_0^2 = gH_0$ respectively measure the strength of the pressure gradient force induced by SST gradients and a barotropic gravity wave speed in the boundary layer; H_0 is the depth of the boundary layer, and T_0 is a reference temperature. In the present study, we set $E = 1/2.5$ day^{-1}, $\epsilon = 1/30$ min^{-1}, $H_0 = 3000$ m, and $T_0 = 288$ K.

The Lindzen–Nigam model neglects the role of convective heating in the free atmosphere and assumes that the atmospheric boundary-layer flow is driven by hydrostatically induced pressure gradients that result from SST gradients through the vertical turbulent mixing of heat and moisture (Wang and Li 1993). In spite of its simplicity, the model is capable of simulating basic features of the seasonally varying low-level winds, particularly in the eastern Pacific.

This atmospheric model makes no allowance for the effects of changes in land surface temperatures, which are known to drive intense monsoons. To test to what extent continents influence the winds over the eastern tropical Pacific, we performed the following experiment: We extended the domain of the model to the global Tropics, included realistic continental geometry, and specified observed seasonally varying sea surface temperatures and land surface temperatures as given by the GFDL climate model (R30) in a 20-year simulation of the seasonal cycle. Although the land temperatures have an enormous effect on the winds over the Indian and tropical Atlantic Oceans, they have, in this model, a very modest effect on the winds over the eastern tropical Pacific. [For a detailed discussion of the effects of continental geometry on winds over the ocean, the reader is referred to Philander et al. (1996).] On the basis of these results we decided to limit the model to the tropical Pacific and to neglect land effects.

The heat flux at the ocean surface depends on the shortwave solar radiation modified by cloudiness. In the eastern tropical Pacific the clouds that have by far the largest effect are the low-level stratus over the cold surface waters off the western coast of the Americas. Klein and Hartmann (1993) discuss observational aspects of these clouds, and Philander et al. (1996) study their role in the time-averaged climate of the Tropics. The clouds are particularly important because they are involved in a positive feedback: the more clouds there are, the lower the sea surface temperature, the larger the atmospheric inversion, and the more clouds there are. In our very simplified model the cloudiness is specified to depend only on sea surface temperature: cloud cover C increases linearly from 0.0 to 0.7 as the sea surface temperature decreases from 29° to 16°C and remains constant (0.7) when the sea surface temperature is below 16°C. This formulation takes into account that evaporation decreases rapidly with a decrease in SST. Where sea surface temperature is high, convective rather than stratus clouds are likely. In our model the effect of stratus clouds is to reduce the shortwave solar radiation in accord with Reed's (1977) expression

$$Q_{\mathrm{SW}} = [Q_0(1 - 0.62C) - \overline{Q_0}(1 - 0.62\bar{C})](1 - \lambda), \tag{2.4}$$

where Q_0 and $\overline{Q_0}$ represent the total and annual-mean solar radiation at the top of atmosphere; C and $\bar{C}$ denote the total and annual-mean cloudiness; and λ denotes the surface albedo, which is taken to be constant (0.06) in the tropical ocean. In (2.4), we have neglected the effect of noon solar altitude. Separate experiments show this to be an unimportant factor.

Evaporation is calculated from the expression

$$Q_{\mathrm{LH}} = \rho_a C_D L[|\mathbf{V} + \bar{\mathbf{V}}|(q_s - q_a) - |\bar{\mathbf{V}}|(\overline{q_s} - \overline{q_a})], \tag{2.5}$$

where $\rho_a = 1.2$ kg m^{-3} is the surface air density; $C_D = 1.3 \times 10^{-3}$ is a drag coefficient; $L = 2.5 \times 10^6$ J kg^{-1} is the latent heat of vaporization per unit mass; and the total and annual-mean sea surface specific humidities, q_s and $\overline{q_s}$, are computed from the sea surface temperature, based on the Clausius–Clapeyron equa-

FIG. 3. Specified time-averaged fields (a) for the sea surface temperature and wind and (b) for surface current and vertical entrainment velocity. Panels (c) and (d) show simulated sea surface temperatures and wind fields in March and September respectively for the reference case in which the model has a rectangular boundary and is forced by the complete seasonally varying solar radiation. The contour intervals are 1°C for SST and 0.0002 m s^{-1} for vertical entrainment velocity. The maximum vectors are 8 m s^{-1} for wind and 40 cm s^{-1} for ocean current.

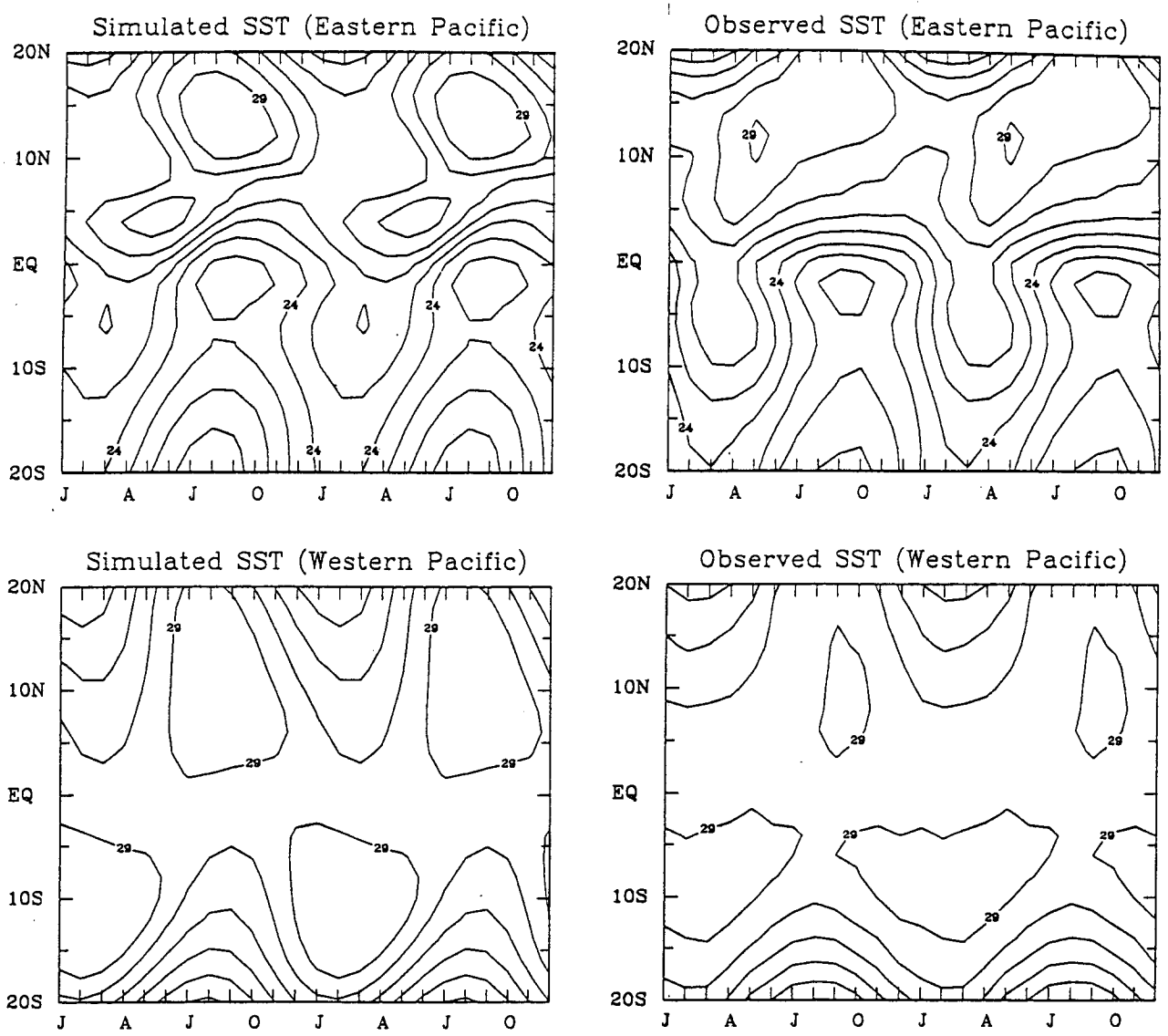

FIG. 4. The annual cycles of sea surface temperatures, simulated and observed, in the eastern Pacific (90°–110°W: upper panels) and in the western Pacific (160°E–180°: lower panels). The model results are from the reference case in which the model is forced with the complete seasonal solar radiation; a realistic, asymmetric annual-mean basic state is specified; and the western coast of the Americas coincides with a meridian.

tion, by assuming a constant annual-mean sea level pressure. The total and annual-mean air specific humidities at the surface, q_a and $\overline{q_a}$, are calculated from SST according to an empirical relationship derived from climatological monthly mean data (see Li and Wang 1994).

This coupled model is similar to that of Zebiak and Cane (1987) and, in response to forcing that corresponds to annual-mean solar radiation, reproduces an interannual Southern Oscillation the way their model does. The key difference between our model and theirs concerns the seasonal cycle. They specify it as part of the given background, whereas in this model it can be calculated, given the time-averaged background state. Recent studies of the interactions between seasonal and interannual variability by Jin et al. (1994), Tziperman et al. (1994), and Chang et al. (1995) indicate that these interactions are complex and are sensitive to changes in parameter values. We have decided to defer further investigation of these issues and to focus on the seasonal cycle and the processes that determine it by suppressing interannual variability in our model. This, fortunately, can be done easily because the air–sea interactions that determine seasonal and interannual variability are very different. Changes in the topography of the thermocline are of central importance to the South-

TABLE 1. Description of model experiments.

Experiment	Description
Reference case	Observed seasonally varying solar radiation; asymmetric time-mean state, rectangular ocean basin, and SST depends on oceanic dynamics and on heat fluxes (including both evaporation and cloud effects).
A	Symmetric annual-harmonic solar radiation, symmetric time-mean state, rectangular ocean basin, and SST as in the reference case.
B	Antisymmetric annual-harmonic solar radiation, symmetric time-mean state, sloping coast in the eastern Pacific, and SST as in the reference case.
C	Antisymmetric annual-harmonic solar radiation, asymmetric time-mean state, rectangular ocean basin, and SST not affected by clouds or evaporation.
D	Antisymmetric annual-harmonic solar radiation, asymmetric time-mean state, rectangular ocean basin, and SST not affected by oceanic dynamics or clouds.
E	Antisymmetric annual-harmonic solar radiation, asymmetric time-mean state, rectangular ocean basin, and SST not affected by clouds.
F	Antisymmetric annual-harmonic solar radiation, asymmetric time-mean state, rectangular ocean basin, and SST as in the reference case.

ern Oscillation but are unimportant to the seasonal cycle. Measurements in the eastern equatorial Pacific, especially the long time series from equatorial moorings, indicate that, seasonally, there is little vertical movement of the thermocline (M. McPhaden 1994, personal communication). Modeling studies by Koeberle and Philander (1994) and Chang (1994) confirm that, whereas interannual sea surface temperature changes are controlled by thermocline movements, seasonal changes are not and depend instead on diabatic processes and on the divergence of surface currents. The interannual variation can therefore be suppressed by keeping subsurface temperatures constant in time in our model. The air–sea interactions that then come into

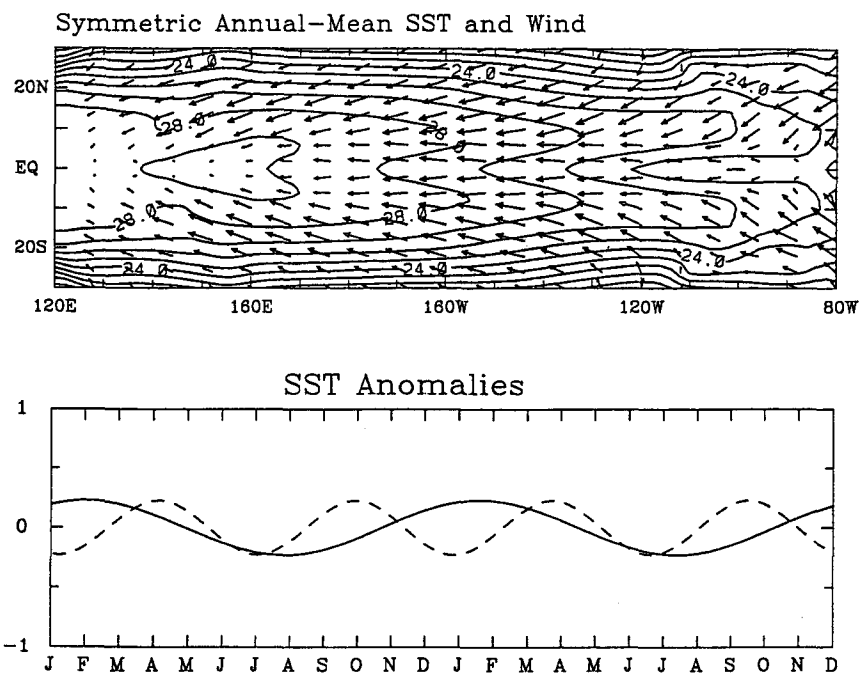

FIG. 5. (a) The symmetric component of climatological annual-mean sea surface temperature and wind fields. (b) The simulated seasonal variations in sea surface temperature at 0°, 100°W from a model forced with the symmetric annual harmonic of the solar radiation (solid line) and with the semiannual harmonic of the solar radiation (dashed line).

play are those studied by Neelin (1991) and Chang and Philander (1994).

Our coupled model was used to make a number of calculations that are listed in Table 1, including a change in the coastal geometry for some of the cases. Where the geometry differs from the actual one so that there is ocean where there ought to be land, we generate background oceanic thermal data by interpolation.

3. Results

In the reference experiment the model is forced with the complete seasonally varying solar radiation, namely the annual harmonic, which has symmetric and antisymmetric components relative to the equator, plus a semiannual harmonic. The model yields results that compare well with the observed fields, as is evident in Fig. 3, which shows the specified time-averaged fields and simulated conditions at the extremes of the seasonal cycle in March and September. Figure 4, which shows the time dependence of sea surface temperatures, establishes that the model captures the essential differences between the seasonal cycles of the western and eastern tropical Pacific. Given that we have a model capable of reproducing a reasonable seasonal cycle, we can now investigate the specific processes that determine the annual harmonic at the equator.

First, we restrict the forcing to be that part of the seasonally varying solar radiation that is strictly symmetric about the equator. For this case (expt A) the Pacific is a rectangular basin and the time-mean state is the symmetric component of the climatological mean state shown in Fig. 5a. The solid line in Fig. 5b shows how the sea surface temperature on the equator at 100°W varies in response to the annual harmonic of solar radiation, the part associated with the ellipticity of the earth's orbit. The phase of this response agrees with that of the observed response—the surface waters are warmest in late northern winter, coldest in summer—but the amplitude is much too small. This component of the forcing by itself cannot explain the observed annual cycle at the equator in the Pacific. To check this statement we can turn to the semiannual signal whose forcing function, associated with the sun crossing the equator twice a year, is as small as the symmetric annual harmonic forcing (see Fig. 6). The response, shown as the dashed line in Fig. 5b, is as small as the response to the annual forcing. This is in agreement with the observed semiannual cycle at the equator except in the central Indian Ocean where the semiannual cycle is enormous, as is evident in Fig. 1. The large semiannual signal of the Indian Ocean emerges as a surprise, and requires an explanation. (This matter will be pursued on another occasion.)

Next we turn our attention to that part of the forcing that is asymmetric about the equator. To cause an annual harmonic at the equator an asymmetry has to be introduced. The first possibility we explore is an asymmetry of the coastal geometry (expt B). [The time-mean state remains symmetric about the equator for the moment. Note that Philander et al. (1996) have demonstrated that asymmetric coastal geometry can cause an asymmetric time-mean state, even when the forcing is symmetric.] Figure 7a shows sea surface temperature variations on the equator at 100°W when the eastern coast of the Pacific coincides with a meridian (the dashed line) and when it is inclined to the coast as in Fig. 7b (the solid line). An inclination of the coast does indeed permit an annual cycle at the equator, with the correct phase but with too small an amplitude. The sloping coast makes a difference for the following reasons: The seasonally varying winds, which are cross equatorial, are toward the summer hemisphere. The Coriolis force deflects them to the right (left) in the Northern (Southern) Hemisphere. If the coast is sloping, as in Figs. 7b and 7c, then the winds have a larger component parallel to the coast in one hemisphere (the Southern) than the other. Hence, the winds induce oceanic upwelling that is more pronounced in one hemisphere than the other. For our particular orientation of the coast (which resembles that of the western coast of the Americas) the Southern Hemisphere has the more pronounced upwelling so that the warmest surface waters are to the north of the equator.

The antisymmetric annual harmonic of solar radiation can force an annual cycle at the equator even when the western coast of the Americas coincides with a me-

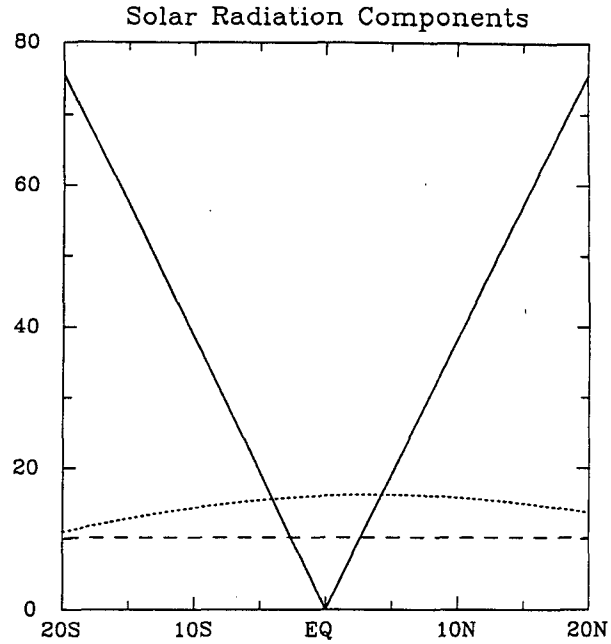

FIG. 6. The latitudinal structure of the amplitude of the antisymmetric annual harmonic (solid line), symmetric annual harmonic (dashed line), and the semiannual harmonic (dotted line) of solar radiation.

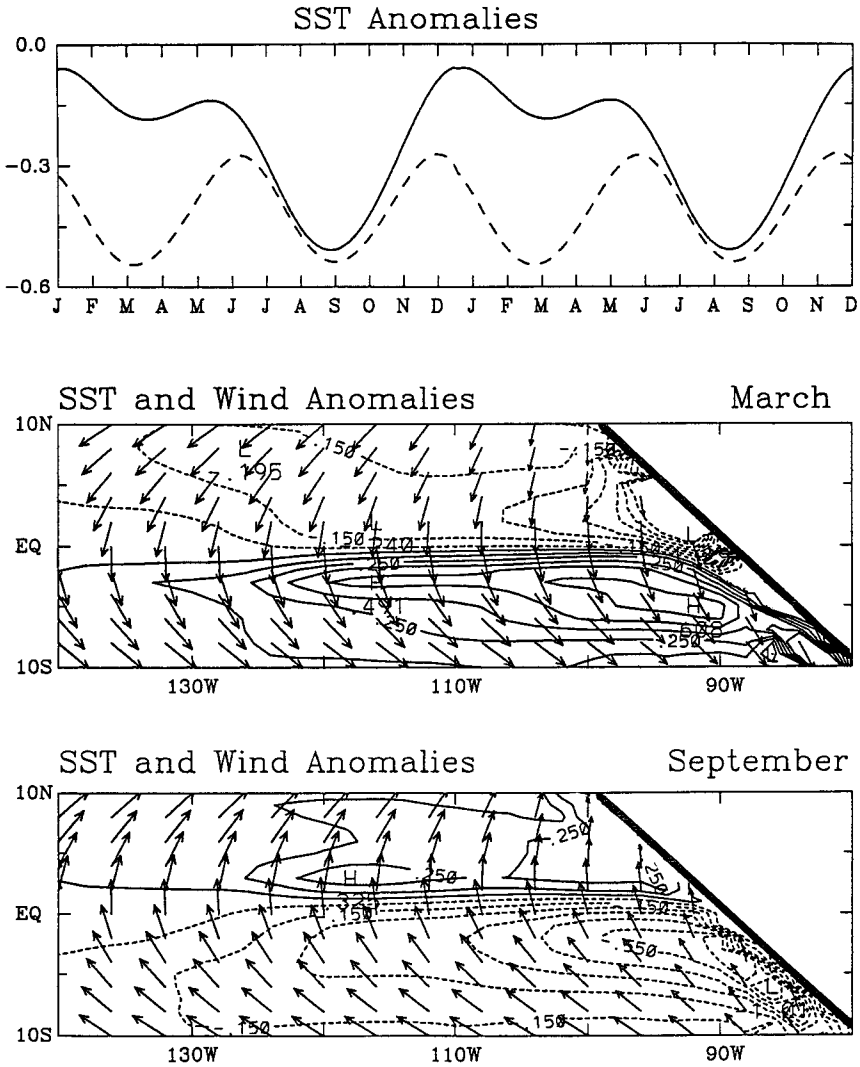

FIG. 7. (a) The time evolution of simulated sea surface temperature anomalies (0°, 100°W) in the presence of a north–south straightline coast (dashed line) and a northwest–southeast sloping coast (solid line). In both cases, a symmetric mean basic state is specified and the forcing is the antisymmetric annual harmonic of solar radiation. The lower panels illustrate the horizontal structure of the anomalous SST and wind fields in (b) March and in (c) September. The maximum wind vector is 1.5 m s^{-1} and the contour interval is 0.1°C.

ridian, provided the time-mean state is asymmetric relative to the equator. We explore this possibility by specifying as our time-mean state the one shown in Figs. 3a,b. Figures 8a shows the latitudinal structure of the response to the strictly asymmetric component of the solar radiation (expt C). (In this case we intensionally suppress the latent heat and cloud effects.) There is clearly an annual cycle in sea surface temperature at the equator. Of central importance is the meridional advection of temperature, the term vT_y, shown in Fig. 8b. The mean meridional temperature gradient $\overline{T_y}$ is positive in the eastern equatorial Pacific (as is evident in Fig. 3a) so that the anomalous advection, which changes direction seasonally, cools the equator during the northern summer and warms it during the northern winter. In other words, the term $v'\overline{T_y}$ leads to an annual cycle at the equator. (Prime indicates an anomalous field.) The term $\overline{v}T_y'$ similarly contributes to an annual cycle because the mean cross-equatorial flow $\overline{v}$ in the eastern equatorial Pacific is northward and because the anomalous meridional temperature gradient T_y' changes sign with the seasons. The vertical advection of temperature is important primarily because it magnifies the meridional temperature gradient; there is downwelling (upwelling) north of (south of) the equator.

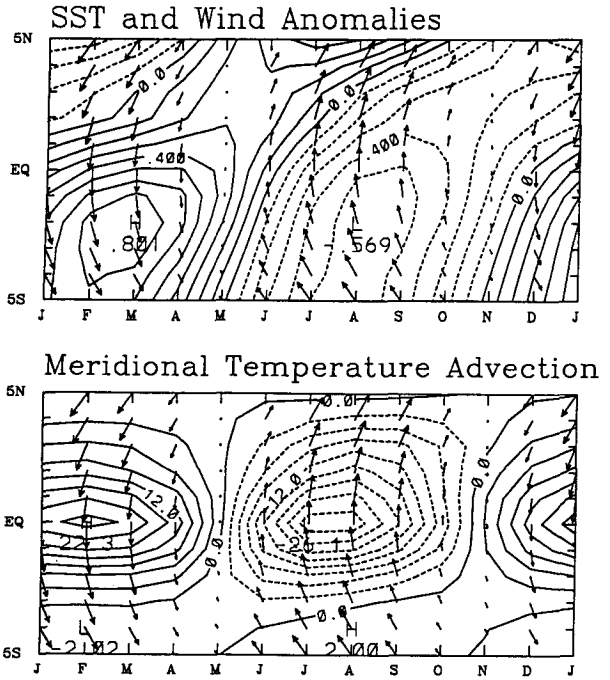

FIG. 8. The time–latitude section of simulated SST and wind anomalies (upper panel) in the eastern Pacific (100°W). In this case, sea surface temperature variations are determined strictly by the dynamic coupling (i.e., wind-induced oceanic upwelling). The thermodynamic coupling, such as latent heat and cloud feedback, is suppressed. The model is forced by a part of solar radiation that is strictly antisymmetric and varies annually. A rectangular ocean boundary is specified. The lower panel shows meridional temperature advection, which converts an antisymmetric SST mode excited by the coupled ocean–atmosphere instability (Chang and Philander 1994) to a symmetric mode and causes the annual change in SST at the equator. The contour intervals are 0.1°C for SST and 3×10^{-8} K s^{-1} for the advection. The maximum wind vector is 2 m s^{-1}.

The results in Fig. 8 show the seasonal cycle that involves the strictly dynamical response of the ocean to the winds. There will be an annual cycle at the equator even if the winds generate no currents but merely cause evaporation, provided the time-mean state has northward winds at the equator (Xie 1994). This is possible because the intensification of those winds during the northern summer and their weakening during the northern winter will cause an annual variation in evaporation and, hence, in sea surface temperature. The dotted line in Fig. 9 (expt D) depicts that variation on the equator at 100°W. It is modest in amplitude, but is magnified if we take into account the combined effects of evaporation and the dynamical response discussed in the previous paragraph and shown in Fig. 8. The solid line of Fig. 9 (expt E) shows this combined effect. Further amplification of the annual harmonic is possible because of the low-level cloud feedback mentioned in section 2 because the lower the sea surface temperatures, the thicker the cloud layer and the smaller the shortwave radiation into the ocean. The dashed line in Fig. 9 (expt F) shows how sea surface temperatures vary when the dynamical response, the evaporation, and cloud feedbacks are all included. This case recovers the seasonal variations of the complete model described at the beginning of this section.

Our calculations indicate that the low-level cloud feedback has little effect on the response to the symmetric annual and semiannual forcing, shown in Fig. 6. This feedback is insignificant when the mean sea surface temperatures are high.

A feature of the annual cycle along the equator is westward phase propagation, at a speed near 50 cm s^{-1}, in the fields of sea surface temperature and zonal wind (Horel 1982). This feature corresponds to a coupled ocean–atmosphere mode of the type investigated by Neelin (1991). Chang and Philander (1994) found that initial perturbations can excite this mode in their coupled model. In our coupled model, forced with seasonally varying solar radiation, westward phase propagation is strikingly evident in the zonal wind field but much less so in the sea surface temperature field. The reasons for this unrealistic aspect of the model are under investigation.

4. Summary and discussion

The eastern equatorial Pacific has a pronounced annual cycle in fields such as sea surface temperature, both components of the surface winds, and cloudiness. The challenge is to explain how the seasonal variations in solar radiation force such a response. The results described in this paper indicate that the annual cycle is forced by the antisymmetric component of the seasonally varying solar radiation. This is possible because of the asymmetry (relative to the equator) of the time-averaged climatic conditions, an asymmetry that is prominent in the eastern tropical Pacific but not the Indian Ocean or western tropical Pacific. That asymmetry permits an annual cycle on the equator, even in a model that couples the atmosphere to a one-dimensional mixed layer ocean. In such a coupled model the northward winds at the equator will be intense toward the end of the northern summer, relaxed toward the end of the southern summer. Evaporation associated with these winds will cause temperatures near the equator to be low in August and September, high in March and April. In other words, the model will have an annual cycle in sea surface temperature at the equator. The amplitude will be modest, but can be augmented by next taking into account the dynamical response of the ocean to the winds: intense northward winds induce upwelling and low sea surface temperatures at and to the south of the equator. Further amplification is possible by including the effects of low-level stratus clouds. They form when cold surface waters lead to an atmospheric inversion and strengthen that inversion by further cooling the surface waters.

In addition to the asymmetric mean state, there are several other factors that contribute to the annual cycle

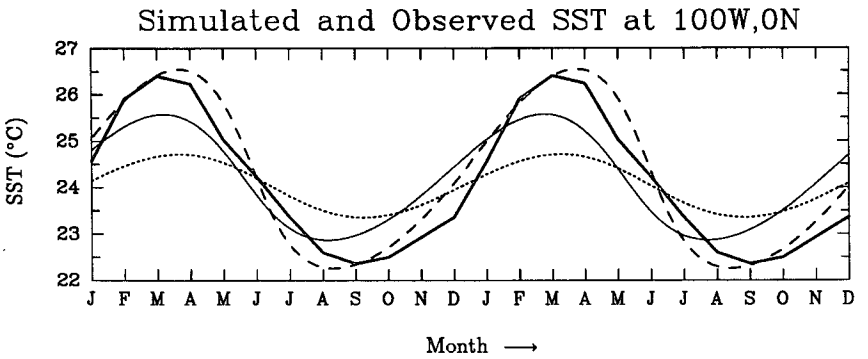

FIG. 9. Seasonal variations of SST at 0°, 100°W in three cases. The SST is determined strictly by evaporation in the case of the dotted line, by evaporation and oceanic upwelling in the case of the solid line, and by evaporation, upwelling, and the presence of low-level stratus clouds in the case of the dashed line. The heavy black line corresponds to the observed variations. In all three cases, a realistic time-mean state that is asymmetric about the equator is specified, the model is forced by part of annually varying solar radiation that is strictly antisymmetric about the equator, and the western coast of the Americas coincides with a meridian.

at the equator. They include the annual cycle in solar radiation associated with the ellipticity of the earth's orbit and the asymmetry, relative to the equator, of the western coastline of the Americas. In our model their contributions are modest and remain so even when ocean–atmosphere interactions and feedbacks associated with low-level clouds are taken into account.

The model used here has the advantages of simplicity and the disadvantages associated with the neglect or oversimplification of important processes. Low-level clouds are grossly oversimplified. Here they depend strictly on sea surface temperature, but in reality they depend on several other factors including atmospheric moisture, atmospheric temperatures (at 850 mb, say), subsidence above the boundary layer, and the speed and direction of the winds. The neglect of land processes restricts the relevance of our calculations to the eastern tropical Pacific. Although processes similar to those discussed here must determine the annual cycle of the equatorial Atlantic, which strongly resembles that of the eastern equatorial Pacific, it is unlikely that the relative importance of the processes remains the same. In calculating the response to the time-mean solar radiation, Philander et al. (1996) found that, in the Atlantic, the bulge of northwestern Africa is of central importance for the climatic asymmetry. It is possible that this bulge is the principal reason for the annual cycle on the equator in the Atlantic. The matter needs to be explored with a more sophisticated coupled model. Other questions that require further study include interactions between the seasonal and interannual variations, and the extent to which the seasonal variations affect the time-averaged state.

Acknowledgments. The authors would like to thank Drs. P. Chang and I. Held for valuable suggestions and discussions. During this study, which was supported by the National Oceanic and Atmospheric Administration (NA26G0102-01) and NASA (NASANAG 5-2224), we had the benefit of access to GFDL computer resources.

REFERENCES

Battisti, D. S., and A. C. Hirst, 1989: Interannual variability in the tropical atmosphere–ocean system: Influence of the basic state and ocean geometry. *J. Atmos. Sci.*, **45,** 1687–1712.

Cane, M. A., 1979: The response of an equatorial ocean to simple wind stress patterns. I: Model formulation and analytic results. *J. Mar. Res.*, **37,** 233–252.

Chang, P., 1994: A study of seasonal cycle of sea surface temperature in the tropical Pacific Ocean using reduced gravity models. *J. Geophys. Res.*, **99**(C4), 7725–7741.

——, and S. G. H. Philander, 1994: A coupled ocean–atmosphere instability of relevance to seasonal cycle. *J. Atmos. Sci.*, **51,** 3627–3648.

——, B. Wang, T. Li, and L. Ji, 1995: Interactions between the seasonal cycle and the Southern Oscillation—Frequency entrainment and chaos in a coupled ocean–atmosphere model. *Geophys. Res. Lett.*, **21,** 2817–2820.

Gill, A. E., 1980: Some simple solutions for heat-induced tropical circulation. *Quart. J. Roy. Meteor. Soc.*, **106,** 447–462.

Halpern, D., 1987: Comparison of upper ocean VACM and VMCM observations in the equatorial Pacific. *J. Atmos. Oceanic Technol.*, **4,** 84–93.

Horel, J. D., 1982: On the annual cycle of the tropical Pacific atmosphere and Ocean. *Mon. Wea. Rev.*, **110,** 1863–1878.

Jin, F.-F., D. Neelin, and M. Ghil, 1994: El Nino on the devil's staircase: annual subharmonic step to chaos. *Science,* **264,** 70–72.

Klein, S. A., and D. L. Hartmann, 1993: The seasonal cycle of low stratiform clouds. *J. Climate,* **6,** 1587–1606.

Knox, R. A., 1981: Time variability of Indian Ocean equatorial currents. *Deep-Sea Res.*, **28A,** 291–295.

Koeberle, C., and S. G. H. Philander, 1994: On the processes that control seasonal variation of sea surface temperature in the tropical Pacific Ocean. *Tellus,* **46A,** 481–496.

Li, T., and B. Wang, 1994: A thermodynamic equilibrium climate model for monthly mean surface winds and precipitation over the tropical Pacific. *J. Atmos. Sci.*, **51,** 1372–1385.

Lindzen, R. S., and S. Nigam, 1987: On the role of sea surface temperature gradients in forcing low level winds and convergence in the tropics. *J. Atmos. Sci.,* **44,** 2440–2458.

Matsuno, T., 1966: Quasi-geostrophic motions in the equatorial area. *J. Meteor. Soc. Japan, Ser. II,* **44,** 25–43.

McPhaden, M. J., and M. E. McCarty, 1992: Mean seasonal cycles and interannual variations at 0°, 110°W and 0°, 140°W during 1980–1991. NOAA Tech. Memo., Contribution No. 1377 from NOAA/Pacific Marine Environmental Laboratory.

Mitchell, T. P., and J. M. Wallace, 1992: On the annual cycle in equatorial convection and sea surface temperature. *J. Climate,* **5,** 1140–1152.

Moore, D. W., and S. G. H. Philander, 1977: Modeling of the tropical oceanic circulation. *The Sea,* E. Goldberg and Coeditors, Wiley-Interscience, 319–361.

Neelin, J. D., 1991: The slow sea surface temperature mode and the fast-wave limit: Analytic theory for tropical interannual oscillation and experiments in a hybrid coupled model. *J. Atmos. Sci.,* **48,** 584–606.

Philander, S. G. H., D. Gu, D. Halpern, G. Lambert, G. Lau, T. Li, and R. C. Pacanowski, 1996: Why the ITCZ is mostly north of the equator. *J. Climate,* **9,** 2958–2972.

Reed, R. K., 1977: On estimating insolation over the ocean. *J. Phys. Oceanogr.,* **7,** 482–485.

Seager, R., S. E. Zebiak, and M. A. Cane, 1988: A model of the tropical Pacific sea surface temperature climatology. *J. Geophys. Res.,* **93,** 1265–1280.

Tziperman, E., L. Stone, M. Cane, and H. Jarosh, 1994: El Niño chaos: Overlapping of resonances between the seasonal cycle and the Pacific ocean–atmosphere oscillator. *Science,* **264,** 72–74.

Wang, B., and T. Li, 1993: A simple tropical atmosphere model of relevance to short-term climate variations. *J. Atmos. Sci.,* **50,** 260–284.

Weingartner, T. J., and R. H. Weisberg, 1991: A description of the annual cycle in sea surface temperature and upper ocean heat in the equatorial Atlantic. *J. Phys. Oceanogr.,* **21,** 83–96.

Xie, S.-P., 1994: On the genesis of the equatorial annual cycle. *J. Climate,* **7,** 2008–2013.

Zebiak, S. E., and M. A. Cane, 1987: A model ENSO. *Mon. Wea. Rev.,* **115,** 2262–2278.